OXFORD

ORIGINAL ARTICLE

KCC2 Manipulation Alters Features of Migrating Interneurons in Ferret Neocortex

F. T. Djankpa[1,2], F. Lischka[3], M. Chatterjee[3] and S. L. Juliano[1,4]

[1]Program in Neuroscience, Uniformed Services University of the Health Sciences, USUHS, Bethesda, MD 20814-4799, USA, [2]Center for the Study of Traumatic Stress, Bethesda, MD 20814-4799, USA, [3]Center for Neuroscience and Regenerative Medicine, USUHS, Bethesda, MD 20814-4799, USA and [4]Anatomy, Physiology and Genetics, Uniformed Services University of the Health Sciences, Bethesda, MD 20814-4799, USA

Address correspondence to Dr Sharon L. Juliano, Professor of Neuroscience, Cellular and Molecular Biology, APG, USUHS, 4301 Jones Bridge Rd., Bethesda, MD 20814-4799, USA, Center for the Study of Traumatic Stress, Bethesda, MD 20814-4799, USA. Email: sharon.juliano@usuhs.edu

Abstract

KCC2 is a brain specific chloride–potassium cotransporter affecting neuronal development including migration and cellular maturation. It modulates chloride homeostasis influencing the switch of GABA from depolarizing to hyperpolarizing, which contributes to the cues that influence the termination of neuronal migration. The expression of KCC2 during migration of interneurons, therefore, correlates with the ability of these cells to respond to GABA as a stop signal. Manipulation of KCC2 in development can affect various aspects of migrating neurons, including the speed. We describe the effect of KCC2 downregulation and inhibition on features of migrating interneurons of normal ferret kits and those treated with methylazoxymethanol acetate, which increases KCC2. Treatment of organotypic cultures with Bisphenol A, an environmental toxin that alters gene expression, also downregulates KCC2 protein. In organotypic slices treated with the KCC2 antagonist VU0240551, chloride imaging shows inhibition of KCC2 via blockade of chloride flux. Time-lapse video imaging of organotypic cultures treated with either drug, shows a significant increase in the average speed, step size, and number of turns made by migrating neurons leaving the ganglionic eminence. Our findings demonstrate the harmful effect of environmental toxins on brain development and potential consequences in the pathogenesis of neurodevelopmental disorders.

Key words: BPA, ganglionic eminence, interneurons, MAM, NKCC1

Introduction

The process of neuronal migration is precisely regulated by numerous factors that ensure proper positioning and functional integrity of the nervous system. During corticogenesis, interneuron precursors generated mainly in the ganglionic eminence (GE) migrate through tangential streams to the cortical plate and then proceed radially using multiple directional cues to reside in the cortical layers (Hatten 2002; Marin and Rubenstein 2003; Rakic 2009; Marin et al. 2010; Miyoshi and Fishell 2011; Poluch and Juliano 2015). Throughout their trajectories a myriad of extracellular molecules such as slits, netrins, semaphorins, and reelin function as guidance cues for migrating interneurons.

Alteration in secretion or expression of these cues misleads the path of the migrating interneurons (Lu et al. 1999; Hatten 2002; Marin et al. 2010; Rudolph et al. 2014).

Several mechanisms stimulate the motility and guide the migration of cortical interneurons. Activation of AMPA receptors leads to neurite retraction during interneuron migration in the intermediate zone of the neocortex (Poluch et al. 2001, 2003). Hepatocyte growth factor functions as a motogen to migrating interneurons in the telecephalon and neuregulin acts as a short and long range attractor for cortical GABAergic interneurons during migration (Flames et al. 2004). Extracellular cues and signaling mechanisms that determine the spatial and

temporal termination of cortical interneuron migration are emerging. Recent evidence suggests that factors secreted by pyramidal cells play important roles in guiding migrating interneurons (Bartolini et al. 2016). In addition, KCC2 influences the termination of interneuron migration into the neocortex through secretion of neuregulin 3 (Bortone and Polleux 2009).

During development, the expression of the ion channels NKCC1 and KCC2 reverses, so that the initially high levels of NKCC1, a chloride importer, decrease, while levels of KCC2, a chloride exporter, increase. The relative levels of these membrane transport proteins determine the developmental switch of GABAergic interneurons from depolarizing (in young neurons) to hyperpolarizing (in mature neurons) (Mueller et al. 1984; Ben-Ari et al. 1989; Delpire 2000; Kahle et al. 2008; Ben-Ari 2014). The expression of KCC2 during migration of interneurons correlates with the ability of these cells to respond to GABA as a stop signal, suggesting that KCC2 might act as a switch controlling GABA from acting in a motogenic capacity to becoming a stop signal in migrating neurons (Bortone and Polleux 2009). KCC2 also influences the final laminar position of interneurons reaching the neocortex (Miyoshi and Fishell 2011). Manipulation of KCC2 expression and/or activity during development can therefore disrupt features of migrating neurons.

We previously observed that administration of methylazoxymethanol acetate (MAM) on embryonic day 33 (E33) induces KCC2 upregulation, which also reduces the speed and alters features of migrating neurons leaving the GE in the ferret (Abbah and Juliano 2014). To determine if the migration defects directly relate to the increased levels of KCC2, we evaluate here the effect of KCC2 downregulation using BPA (2,2-bis-(4-hydroxy-phenyl) propane) and KCC2 antagonism (using the KCC2 antagonist VU0240551) on normal P0 cerebral cortex and on neocortex treated with MAM (which normally shows increased KCC2 levels).

Our findings indicate that exposure to environmental toxins such as BPA can affect brain development. We also show that optimal expression and function of KCC2 is indispensable for the integrity of neuronal migration during corticogenesis in ferrets.

Materials and Methods

Ethics Statement

All experiments in this work were done in accordance with the guidelines approved by the Institutional Animal Care and Use Committee (IACUC) at the Uniformed Services University of the Health Sciences (USUHS).

Animals and MAM Injection

Timed pregnant ferrets (*Mustella putorius furo*) were purchased from Marshall Farms (New Rose, NY). At embryonic day 33 (E33), pregnant ferrets were anesthetized with 5% isofluorane using a mask and given an intraperitoneal (IP) injection of methylazoxymethanol acetate (MAM, MRI Global, Kansas City, MO), at a dose of 14-mg/kg diluted in sterile 0.9% sodium chloride (Hospira Inc, Lake Forest, IL). MAM-treated pregnant jills were allowed to recover and gestation proceeded until 41 days when ferret kits are normally born. The total number of normal and MAM treated jills used is summarized in Table 1.

Preparation of Organotypic Slices

We prepared organotypic slice cultures as previously described (Palmer et al. 2001; Abbah and Juliano 2014). Postnatal day 0 (P0) ferret kits were anesthetized with sodium pentobarbital (50 mg/kg, IP); when insensitive to pain, we removed their brains and placed them in ice-cold artificial cerebrospinal fluid (ACSF) composed of $NaCl^-$ (124 mM), KCl^- (3.2 mM), $CaCl_2^-$ (2.4 mM), $MgCl_2^-$ (1.2 mM), $NaHCO_3$ (26 mM), NaH_2PO_4 (1.2 mM), and 10 mM glucose and bubbled with 95% O_2 and 5% CO_2 under a laminar flow hood. Coronal slices (500 μm thick) were prepared from each hemisphere using a tissue chopper (Stoelting, Co., Wood Dale, IL, USA). Brain slices were transferred into 0.4 μm culture plate inserts (Millicell-CM, Bedford, MA, USA) placed in 6-well plates containing Minimum Eagles Medium, MEM, (GIBCO, Gaithersburg, MD) and supplemented with 10% horse serum (GIBCO, Gaithersburg, MD) and 4% G 1:2 (containing gentamycin and glutamine). Slices were incubated at 37 °C under 5% CO_2. The total number of kits is summarized in Table 1.

KCC2 Manipulation

BPA (Sigma Aldrich, St. Louis, MO) was dissolved in DMSO (Sigma Aldrich ≥ 99%) to a concentration of 50 nM with the DMSO final concentration being less than 0.01% in the medium as recommended by the manufacturer. The KCC2 antagonist VU0240551 (Sigma Aldrich, St. Louis, MO) was added to the medium to a final concentration of 1 or 5 μM and added to the organotypic cultures. Our final concentration of DMSO was added to the medium alone and used in a set of organotypic cultures for western blots to determine its independent effect.

MEQ (6-Methoxy-N-Ethylquinolinium Iodide) Chloride Imaging

The MEQ chloride imaging was carried out according to standard protocol as previously described (Biwersi and Verkman 1991; Schwartz and Yu 1995; Inglefield and Schwartz-Bloom 1999). The MEQ was reduced to a cell-permeable form, 6-methoxy-N-ethyl-1,2-dihydro-quinoline (DiH-MEQ), by dissolving 5 mg of MEQ in 0.1 mL of distilled water in a glass test tube placed under a stream of N_2, and adding 12% sodium boratehydride ($Na_2B_4O_7 \cdot 10H_2O$). The resulting solution was kept under a stream of N_2 for 30 min until an oily yellow substance forms. Distilled water and ethyl acetate (0.5 mL each) were then added to the reaction tube, vortexed and the solution allowed to separate into aqueous and organic layers. The organic layer (top) containing DiH-MEQ was carefully separated with a pipette and placed in a fresh tube. This step was repeated and the 2 organic layers combined and dehydrated by adding 100 mg of anhydrous magnesium sulfate ($MgSO_4$). After 5 min, the organic layer was transferred with a pipette into a glass microvial and the ethyl acetate evaporated with a stream of N_2. DiH-MEQ was freshly prepared before each experiment and dissolved in 10 mL ACSF immediately before dye loading. The slices, cut as described above, incubated for 30 min in the DiH-MEQ solution and allowed to absorb the dye. The initial florescence (F_0) intensity was recorded with a Zeiss 7 Multiphoton microscope equipped with Zen-2012 software (black edition). While recording continuously, the VU0240551 was added at 2 different times at a concentration of 1 or 5 μM and the fluorescence intensity (F) recorded. Graphs were plotted with normalizing fluorescence intensity by dividing by baseline F_0 to compare the amplitude of change between cells. DiH-MEQ is quenched in the presence of chloride, thus a decrease in fluorescence corresponds to an increase in intracellular chloride concentration. The change in intracellular chloride concentration following

Table 1. Number of jills and ferret kits used for slice culture and live imaging experiments

Jills	Number of kits used	Treatments
F1 Normal	1 P0 kit	Control (medium), Vehicle (medium +DMSO) on different slices
	1 P0 kit	Treated with BPA (50 and 100 nM)
	2 P0 kits	Treated with KCC2 antagonist (1 and 5 μM)
F2 Normal	1 P0 kit	Control, Vehicle, BPA-50 nM and 100 nM, KCC2 antagonist 1 μM, and 5 μM.
	1 P0 kit	Control, Vehicle, BPA-50 nM and 100 nM KCC2 antagonist 1 μM, and 5 μM.
	1 P0 kit	Control, Vehicle, BPA-50 nM and 100 nM, KCC2 antagonist 1 μM, and 5 μM.
	1 P0 kit	Control, Vehicle, BPA-50 nM and 100 nM, KCC2 antagonist 1 μM, and 5 μM.
F3 Normal	1 P0 kit	Control, Vehicle, BPA-50 nM and KCC2 antagonist 5 μM.
	1 P0 kit	Control, Vehicle, BPA-50 nM and KCC2 antagonist 5 μM.
	1 P0 kit	Control, Vehicle, BPA-50 nM and KCC2 antagonist 5 μM.
	1 P0 kit	Control, Vehicle, BPA-50 nM and KCC2 antagonist 5 μM.
F4 Normal	1 P0 kit	Control, Vehicle, BPA-50 nM and KCC2 antagonist 5 μM.
	1 P0 kit	Control, Vehicle, BPA-50 nM and KCC2 antagonist 5 μM.
	1 P0 kit	Control, Vehicle, BPA-50 nM and KCC2 antagonist 5 μM.
	1 P0 kit	Control, Vehicle, BPA-50 nM and KCC2 antagonist 5 μM.
F4 Normal	1 P0 kit	Control, Vehicle, BPA-50 nM and KCC2 antagonist 5 μM.
	1 P0 kit	Control, Vehicle, BPA-50 nM and KCC2 antagonist 5 μM.
	1 P0 kit	Control, Vehicle, BPA-50 nM and KCC2 antagonist 5 μM.
	1 P0 kit	Control, Vehicle, BPA-50 nM and KCC2 antagonist 5 μM.
F5 Normal	1 P0 kit	Control, Vehicle, BPA-50 nM and KCC2 antagonist 5 μM.
	1 P0 kit	Control, Vehicle, BPA-50 nM and KCC2 antagonist 5 μM.
	1 P0 kit	Control, Vehicle, BPA-50 nM and KCC2 antagonist 5 μM.
	1 P0 kit	Control, Vehicle, BPA-50 nM and KCC2 antagonist 5 μM.
F6 E33 MAM	1 P0 kit	Control, Vehicle, BPA-50 nM and 100 nM, KCC2 antagonist 1 μM, and 5 μM.
	1 P0 kit	Control, Vehicle, BPA-50 nM and 100 nM, KCC2 antagonist 1 μM, and 5 μM.
	1 P0 kit	Control, Vehicle, BPA-50 nM and 100 nM, KCC2 antagonist 1 μM, and 5 μM.
	1 P0 kit	Control, Vehicle, BPA-50 nM and 100 nM, KCC2 antagonist 1 μM, and 5 μM.
F7 E33 MAM	1 P0 kit	Control, Vehicle, BPA-50 nM, and KCC2 antagonist 5 μM.
	1 P0 kit	Control, Vehicle, BPA-50 nM, and KCC2 antagonist 5 μM.
	1 P0 kit	Control, Vehicle, BPA-50 nM, and KCC2 antagonist 5 μM.
	1 P0 kit	Control, Vehicle, BPA-50 nM, and KCC2 antagonist 5 μM.
F8 E33 MAM	1 P0 kit	Control, Vehicle, BPA-50 nM, and KCC2 antagonist 5 μM.
	1 P0 kit	Control, Vehicle, BPA-50 nM, and KCC2 antagonist 5 μM.
	1 P0 kit	Control, Vehicle, BPA-50 nM, and KCC2 antagonist 5 μM.
	1 P0 kit	Control, Vehicle, BPA-50 nM, and KCC2 antagonist 5 μM.

KCC2 inhibition was estimated using the Stern–Volmer equation, as previously described (Krapf et al., 1988; Verkman 1990; Inglefield and Schwartz-Bloom 1999). Our experiments were performed at 23 °C and the Stern–Volmer constant for chloride ion at that temperature was estimated to be $Kq = 16\,M^{-1}$ (Inglefield and Schwartz-Bloom 1999).

Western Blotting

Treated organotypic slices were snap frozen on dry ice after 5 h in culture (for VU0240551) and 24 h (for BPA). For protein extraction, the frozen samples were thawed on ice and homogenized in ice-cold RIPA lysis buffer supplemented with sodium orthovanadate, protease inhibitors and PMSF (Santa Cruz Biotechnology, Dallas, TX). All homogenization was done by sonication at 4 °C, followed by centrifugation at 4 °C in an Eppendorf centrifuge 5415 C at 20, 000 rpm for 30 min. The supernatants were collected and protein concentrations determined using the bicinchoninic acid (BCA) protein assay method (Thermo Scientific, Pittsburgh, PA).

Protein samples were denatured by addition of Nupage SDS sample buffer and Nupage sample reducing agent (Invitrogen, Grand Island, NY) and heating at 70 °C for 10 min. Electrophoresis of the cation-chloride transporter (KCC2) was accomplished using NUPAGE Novex 3–8% Tris-Acetate gel and NUPAGE Tris-Acetate SDS running buffer supplemented with NUPAGE antioxidant (Invitrogen, Grand Island, NY) and 40 μg of protein loaded in each well. Electrophoresis for the methyl-CpG-binding protein2 (MeCP2) was accomplished using the NUPAGE Novex 10 Bis-Tris gel and NUPAGE Bis-Tris running buffer supplemented with NUPAGE antioxidant (Invitrogen, Grand Island, NY) and 40 μg of protein loaded in each well. Proteins were transferred onto 0.45 μm-pore nitrocellulose membranes using the iBlot dry blotting system (Invitrogen, Grand Island, NY). Membranes were blocked for 1 h at room temperature in 5% milk blocking buffer dissolved in 1X TBS supplemented with 0.1% Tween-20 (Bio Rad, Hercules CA) and incubated with rabbit polyclonal anti-KCC2 (1:500, Millipore, Billerica, MA), at 4 °C overnight. The next day, membranes were washed repeatedly in TBS-Tween solution and incubated in goat antirabbit secondary antibody conjugated to horseradish peroxidase (Invitrogen, Grand Island, NY, 1:2000) diluted in TBS-Tween, followed by detection using enhanced chemiluminescence reagents (PerkinElmer, Melville, NY). The bands were quantified using ImageJ software (https://imagej.nih.gov/ij/) and the densities compared across different conditions using a one-way ANOVA followed by the Tukey post hoc multiple comparison test.

Cell Labeling

We used electroporation to focally transfect cells within the ventricular zone (VZ) in vitro as described previously (Abbah and Juliano 2014). Briefly, transfection was accomplished using a plasmid that codes for red fluorescent protein (RFP), which was cloned into pCAGGS expression vector (a gift from Dr Tarik Haydar). Between 4 and 5 μL of plasmid DNA (1–2 μg/μL) was injected onto the GE surface of the organotypic slices. The cathode of a gene paddle electrode (Harvard Apparatus, Inc., Holliston, MA) was placed within the lateral ventricle close to the VZ of the GE while the anode was positioned close to the pial surface in an appropriate position. A pulse of 60 V was applied 4 times, each for 50 ms at intervals of 950 ms using a BTX ECM830 pulse generator (Harvard Apparatus, Inc., Holliston, MA) (Gal et al. 2006). Slices were incubated as above for at least 24 h prior to video imaging.

Video Imaging

After incubating the organotypic slices for 24–48 h, migrating neurons were continuously visualized using an Axiovert 200 inverted microscope fitted with an apotome and Axiovision software (Carl Zeiss AG, Oberkochen, Germany). The microscope was also fitted with an incubation chamber and a holder for the slices, which were maintained with humidification at 37 °C and 5% CO_2. Serial stacks of images taken through the thickness of the slice were collected using a ×10 objective every 30 min for 24 h using Zen software (black edition). The image stacks were collapsed into a single frame prior to analysis of migration. Migrating cells leaving the GE were analyzed after crossing the corticostriatal boundary into the neocortex.

Analysis of Migration

To measure speed, we tracked migrating cells captured in real time using the M-trackJ plugin of the FIJI package of imageJ software (https://imagej.nih.gov/ij/). The initial data captured included the tracked distances, the travel time, the speed of movement and the angles of turn of neurons. These data were extracted and analyzed using Graph Pad Prism version 6 software. We captured the data at 30 min intervals with each interval representing a frame. For the average speed, we computed the mean across frames and grouped the data in categories to find the mean in each category. A Student's *t*-test was used to compare 2 means for most assessments. For the analysis of the speed over time we used a 2-way analysis of variance (ANOVA) followed by a Sidak post hoc test for multiple comparisons, with the level of confidence set at $P < 0.05$.

Results

Experimental Design and Cell Labeling

In brains with increased levels of KCC2, interneurons migrating into the cerebral cortex move more slowly and show lowered amounts of exploratory behavior (Abbah and Juliano 2014; Abbah et al., 2014). To test whether this abnormal behavior is specifically due to the presence of increased KCC2, we used 2 methods to reduce the activity of this chloride transporter protein. In this study, organotypic cultures containing the GE were labeled using electroporation. We used the same cell labeling technique (in vitro electroporation) as previously described to visualize and track migrating interneurons leaving the GE toward the neocortex (Abbah and Juliano 2014). Figure 1 shows

electroporated cells in organotypic slices that are migrating en route to the neocortex, in a normal ferret (Fig. 1A) and in a MAM-treated ferret (Fig. 1B). For one method to block the effects of KCC2, we added bisphenol A (BPA) to the organotypic cultures, which reduces KCC2 mRNA and subsequent production of KCC2. For the second method we used a pharmacologic antagonist, VU0240551, thereby blocking the activity of KCC2 but not altering its production. After each treatment, we evaluated the migration pattern of labeled cells leaving the GE. For each situation we monitored features of migration and movement of the labeled cells.

KCC2 Downregulation With BPA Affects Features of Interneurons Migrating Away From the GE

The effect of BPA on brain development and function is substantial (Negri-Cesi 2015). BPA downregulates KCC2 mRNA and protein levels in neurons (Yeo et al. 2013). Gestational E33 MAM treatment upregulates KCC2, which correlates with decreased speed and altered migratory features of interneurons leaving the GE (Abbah and Juliano 2014). Concentrations of 50 and 100 nM BPA reduce KCC2 levels in cultured neurons or organotypic cultures (Yeo et al. 2013). We initially observed that 50 nM BPA supported optimal viability of neurons in slices, while
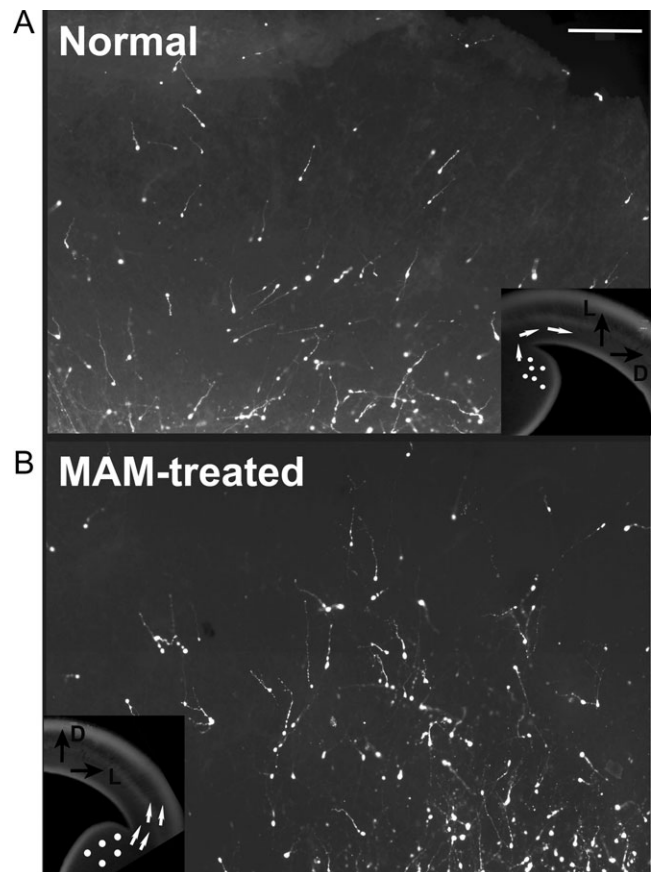

Figure 1. Immunostaining of electroporated organotypic cultures. Electroporated organotypic slices expressing RFP (enhanced by immunohistochemistry) show migrating neurons moving from the ganglionic eminence (GE) to the neocortex. (A) Normal slice, (B) E33 MAM treated slice. The insets in (A) and (B) show the approximate positions of the electroporated cells in the GE (white circles) and the path of the migrating cells indicated by white arrows. The orientation of the slices is indicated by the black arrows; D, dorsal; L, lateral. Scale: 200 μm.
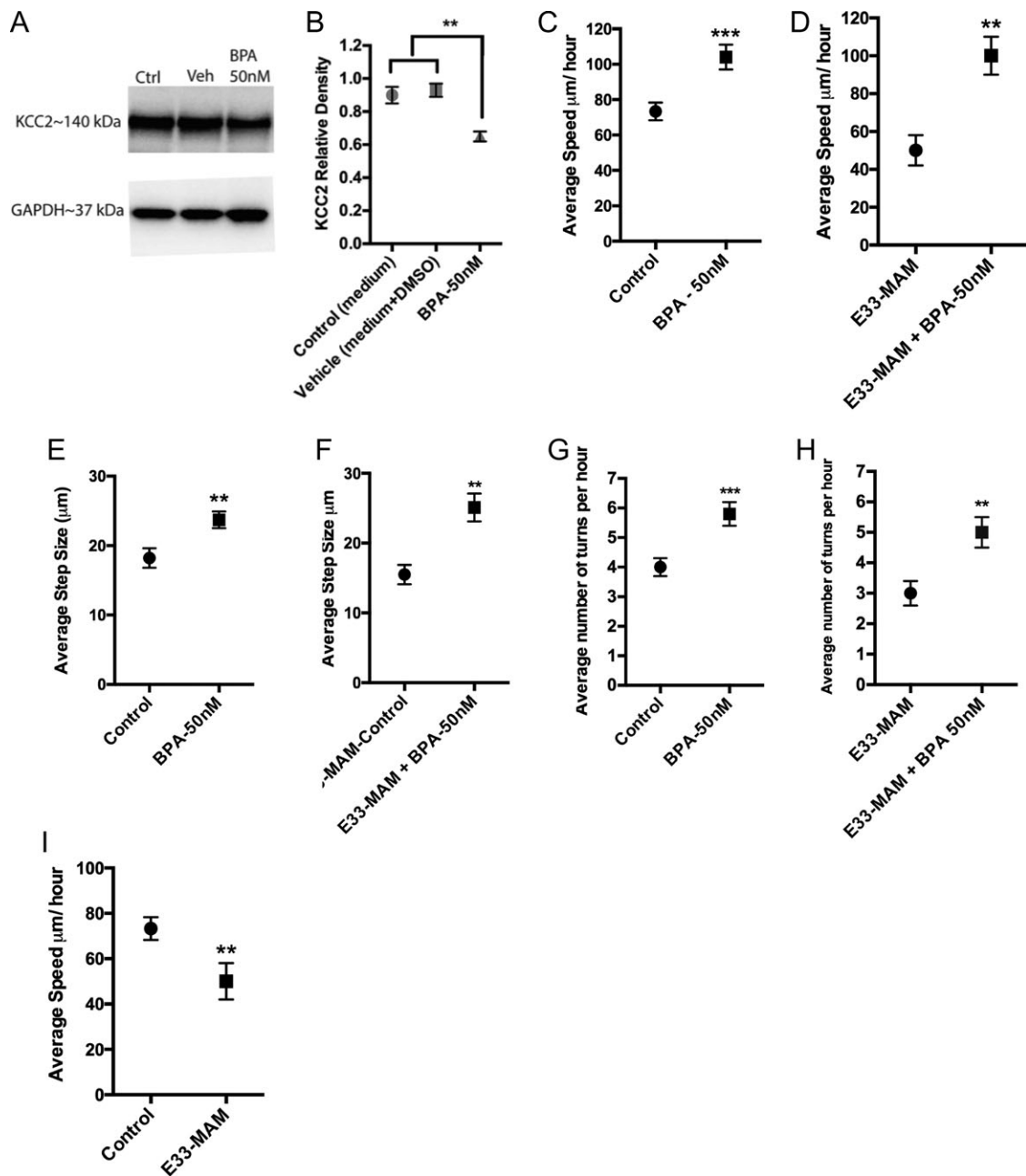
Figure 2. Effect of BPA on KCC2 protein levels and features of migrating neurons. (A) BPA treatment for 24 h significantly decreases KCC2 protein levels as seen in this western blot. (B) The quantification obtained for 3 animals in each group, $F(2, 6) = 14.18$, ANOVA followed by a Tukey post hoc multiple comparison test, $**P < 0.01$. (C, D) BPA treatment significantly increases the speed of migrating neurons in control ferrets and in organotypic cultures obtained from E33 MAM treated kits, Student's t-test $**P < 0.01$. (E, F) BPA treatment also increases the average step size of migrating neurons in control ferret organotypic cultures and in E33 MAM treated slices, Student's t-test, $**P < 0.01$. (G, H) BPA treatment increases the number of turns of migrating neurons in normal and E33 MAM treated ferret organotypic cultures, Student's t-test, $**P < 0.01$, $***P < 0.001$. (I) E33 MAM treatment significantly decreases the speed of migrating neurons leaving the ganglionic eminence in ferret neocortex Student's t-test $**P < 0.01$. N = 102 neurons (Control), 67 neurons (Control + BPA-50 nM), 5 neurons (E33-MAM), and 6 neurons (E33-MAM + BPA).

100 nM induced a level of toxicity so that the slices appeared unhealthy after 24 h in culture. As a result, to test the causality between KCC2 levels and the speed of migrating neurons, we treated organotypic cultures with 50 nM BPA. Since KCC2 slows the speed of migrating interneurons (Bortone and Polleux 2009), we predicted that a decrease in KCC2 levels would increase the speed of migrating neurons in our preparation. To initially determine the effect of BPA on levels of KCC2 we conducted western blots on the tissue taken from the organotypic cultures treated with BPA or with vehicle (medium + DMSO) after 24 h. BPA treatment decreases KCC2 protein levels significantly compared with control but DMSO alone has no detectable effect on KCC2 protein levels (Fig. 2A,B). We next studied the effect of BPA on the migratory speed of neurons leaving the GE. After adding 50 nM of BPA to the medium of prepared slices, each cultured slice received electroporation into the GE with RFP. Following incubation for 24 h, we imaged each slice for an additional 24 h at 30-min intervals. We defined the distance a
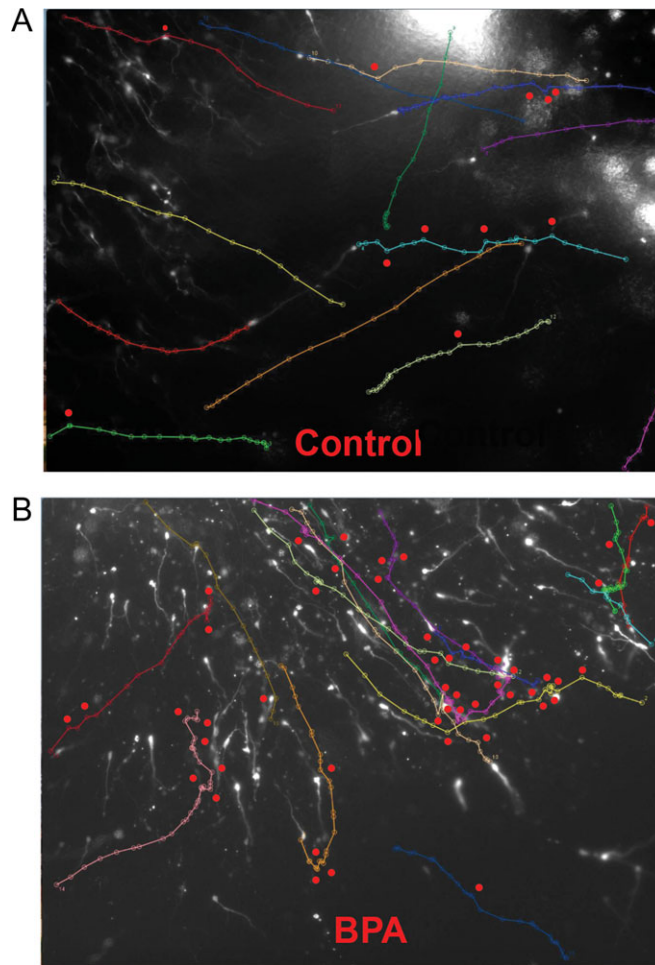
Figure 3. Examples of the tracks of cells that migrate in control and BPA treated cultures. (A) This image shows the path of selected cells in control slices migrating over a period of 5 h. Each cell is indicated in a different color and every point at which a cell makes a turn is indicated with a red dot. (B) This shows the tracks of cells in a slice treated with Bisphenol A (BPA). Each location that a cell makes a turn is indicated with a red dot.

neuron moved during a 30 min interval as a "step". The length of each step was captured and expressed as the "step size." The analysis over the 24 h of migration showed a significant increase in the speed and step size of migrating neurons from the normal cultures treated with 50 nM BPA compared with control (Fig. 2C,E). When the slices treated with E33 MAM were evaluated, we found the migration speed of those receiving BPA to be significantly increased (Fig. 2D,F). Figure 2I shows the average speed compared between control slices and those from E33 MAM treated ferrets. We found previously that MAM treatment upregulates KCC2 protein levels and consequently decreases the speed of migrating neurons (Abbah and Juliano 2014). Similarly, Figure 2I shows that the average speed in control slices is significantly higher than that in E33 MAM treated slices, as we demonstrated previously.

Movie 1 (Movie 1—Control neurons) shows the migration behavior of control neurons. Cells can be seen moving with an overall trend toward the neocortex but migrating neurons travel in multiple directions and show turns in unique trajectories. See Supplemental Figure S1 for schematics of the site each Movie was captured. Our previous studies revealed that organotypic slices receiving MAM treatment (producing increased levels of KCC2), show decreased numbers of turns as the neurons move toward the neocortex (Abbah and Juliano 2014). As we see in Figure 2A,B that treatment with BPA reduces KCC2,

we assessed the number of turns made by migrating cells in control cultures and those treated with BPA. To measure the turns, we used the "track changes" plugin in Fuji (ImageJ) to reveal the path of cells as they moved. Figure 3 shows the traces of neurons created in Fiji that reveal the path of cells that were studied for at least 5 h of movement. Each turn was measured when a cell changed its path of movement by at least 30° and is indicated in this figure as a red dot. Movie 2 (Movie 2 —Tracks of control neurons) indicates the path of individual cells as they traveled in control slices. BPA treatment significantly increases the number of turns made by neurons per hour in the course of migration compared with control (Figs 2G and 3) and this is also true for E33 MAM slices treated with BPA (Fig. 2H). Movie 2 (Movie 2—Tracks of neurons in control slices in BPA-treated slices) indicates the paths of neurons in a control slices and the turns made; Movie 3 (Movie 3—Tracks of neurons in BPA-treatment) shows the tracks of neurons migrating in BPA treated slices. See Supplemental Figure S1 to view schematics of the site for each Movie.

Overall, we find that adding BPA to organotypic cultures reduces KCC2 levels and increases the speed, step size and number turns made by cells migrating away from the GE.

Since we knew treatment with MAM resulted in increased KCC2, we wondered if it also caused changes in substances that influence KCC2 expression and on overall DNA methylation. To

test this, we carried out 2 preliminary experiments to evaluate the interrelation between MeCP2, KCC2, and overall DNA methylation. We conducted western blots to reveal levels of MeCP2 in normal and MAM-treated cortex to assess these relationships. We also used a methylation kit to measure overall methylation in a control and MAM treated brain, both at P0. We show in Supplemental Figure S2 that MAM treatment results in increased levels of MeCP2 and overall increased methylation levels in the brain of a MAM treated animal.

Validation of KCC2 Antagonist (VU0240551) Using MEQ Chloride Imaging

KCC2 inhibition was achieved by application of the antagonist VU0240551 and confirmed with the MEQ chloride imaging. The KCC2 antagonist VU0240551 selectively and specifically inhibits KCC2 by binding competitively to the K^+ site and noncompetitively to the Cl^- site in the KCC2 active region thereby hindering chloride flux. Various methods successfully demonstrate KCC2 inhibition by this antagonist (Delpire et al. 2009; Deisz et al. 2014). To verify that VU0240551 blocked Cl^- movement, we used MEQ chloride imaging on slices similar to those used to study migration. In the MEQ chloride imaging shown in Figure 4, the fluorescence is quenched by chloride ions entering the cell, resulting in an inverse relationship between intracellular $[Cl^-]$ and fluorescence intensity. Higher fluorescence intensity in a given cell corresponds to a lower intracellular $[Cl^-]$ and vice versa. Figure 4A shows neocortical neurons filled with the dye MEQ; Figure 4B,C indicates there is no bleaching of the dye because after 15 min of recording, the fluorescence intensity does not diminish. Figure 4C presents a magnification of the area imaged for 15 min outlined with the square in Figure 4B. Application of the KCC2 antagonist at 1 and 5 μM concentrations decrease the fluorescence intensity indicating an increase in intracellular $[Cl^-]$, which restores when the antagonist is washed out (Fig. 4D). We estimated the change in intracellular chloride concentration using the Sterm–Volmer equation; the results shown in Figure 4E reveal a ~10 mM increase in intracellular chloride concentration corresponding to the change in fluorescence intensity in Figure 4D. We estimated the increase in intracellular chloride concentration in 16 neurons and plotted their values and the average change (Fig. 4F). The increase in intracellular chloride concentration varied between 3.1–10.5 mM with an average of 6.0 mM $\pm$ 0.5 (SEM). The fluorescence intensity during application of the antagonist was normalized to baseline recording (without the antagonist) so that each cell served as its own control (before and after treatment with the antagonist) as shown in Figure 4D.

Effect of KCC2 Inhibition on Features of Migrating Neurons Leaving the GE

After successful inhibition of KCC2 protein activity in organotypic slices we evaluated the migratory behavior of inhibitory neurons using live imaging. Under certain circumstances (not fully understood) KCC2 can be degraded through calcium activated protease calpain and it is possible that long term inhibition of KCC2 by its antagonist VU0240551 could lead to degradation of the KCC2 protein (Puskarjov et al. 2012; Deisz et al. 2014). In order to ensure the integrity of KCC2 protein in the organotypic cultures we conducted western blots 5 h after treatment of the organotypic slices with the KCC2 antagonist. Our choice of 5 h for the treatment was informed by previous findings that the MEQ dye stayed inside the cell up to 4 h

(Inglefield and Schwartz-Bloom 1999). Figure 5A,B shows the antagonist has no effect on KCC2 protein levels after 5 h of incubation. Analysis of live imaging of the slices treated with 5 μM KCC2 antagonist for 5 h shows an increase in the average speed as well as the average step size of cells leaving the GE as shown in Figure 5C,E. The increase in migration speed is also significant for the E33 MAM slices treated with the KCC2 antagonist (Fig. 5D,F). Movie 4 shows the migration behavior of neurons in slices treated with the KCC2 antagonist.

Variability of Speed of Migrating Neurons Over Time

Movie 1 shows that interneurons leaving the GE move in multiple directions and they often make turns. Some cells also move for a time and then remain in the same place without a specific direction (e.g., see Movie 4). Our assessment of migratory speed focused entirely on the time during which the cells moved without including the times they stopped and explored the environment. We find that with treatment of BPA and the KCC2 antagonist the average speed of cells leaving the GE increases overall. Because substantial unevenness in the overall pattern of movement occurs, we assessed cells that moved continuously over a period of 5 h and evaluated the average speed variability over time. We computed the average speed across the time frames and focused on neuronal migration for this time block because we know the KCC2 antagonist does not degrade KCC2 protein levels for at least 5 h of treatment (Fig. 6A,B). Figure 6A,B shows the speed–time graphs for BPA and KCC2 antagonist treatment. Figure 6A shows that the migration speed of neurons treated with BPA generally exhibits a gradual increase over the period studied, but displays some variability over the 5-h period. The speed of the BPA treated neurons is typically significantly higher than that of control neurons at all time points except between the second and third hour. Figure 6B shows that after treatment with the KCC2 antagonist, the migration speed increases gradually until the third hour of migration and then decreases slightly, while remaining significantly greater than the control migration speeds until the last time point.

Summary of Findings

Neuronal migration is intricately fine-tuned by a myriad of factors (both internal and external) to attain the normal cytoarchitecture needed for proper function of the brain (Marin 2003; Marin and Rubenstein 2003; Fishell and Kriegstein 2005; Marin et al. 2010). We reported earlier that gestational delivery of MAM (an environmental toxin) on E33 upregulates KCC2 protein, which correlates with decreased speed and altered behavior of migrating interneurons leaving the GE in ferret neocortex (Abbah and Juliano 2014). Here we show that downregulation of KCC2 through another environmental toxin (BPA) and a KCC2 antagonist counteracts the abnormal features of neuronal migration observed after increases in KCC2.

BPA treatment in organotypic slices at a dose of 50 nM for 24 h significantly downregulates KCC2 protein to result in increased speed and step size of migrating interneurons leaving the GE compared with control migrating neurons. Similarly, treatment of organotypic slices with 1 and 5 μM of the KCC2 antagonist VU0240551 inhibits KCC2 activity by limiting chloride flux. This also correlates with increased speed and step size of migrating neurons. Reducing the effect of KCC2 (with BPA or an antagonist) tends to counteract the effect of MAM treatment and increases the migration speed.
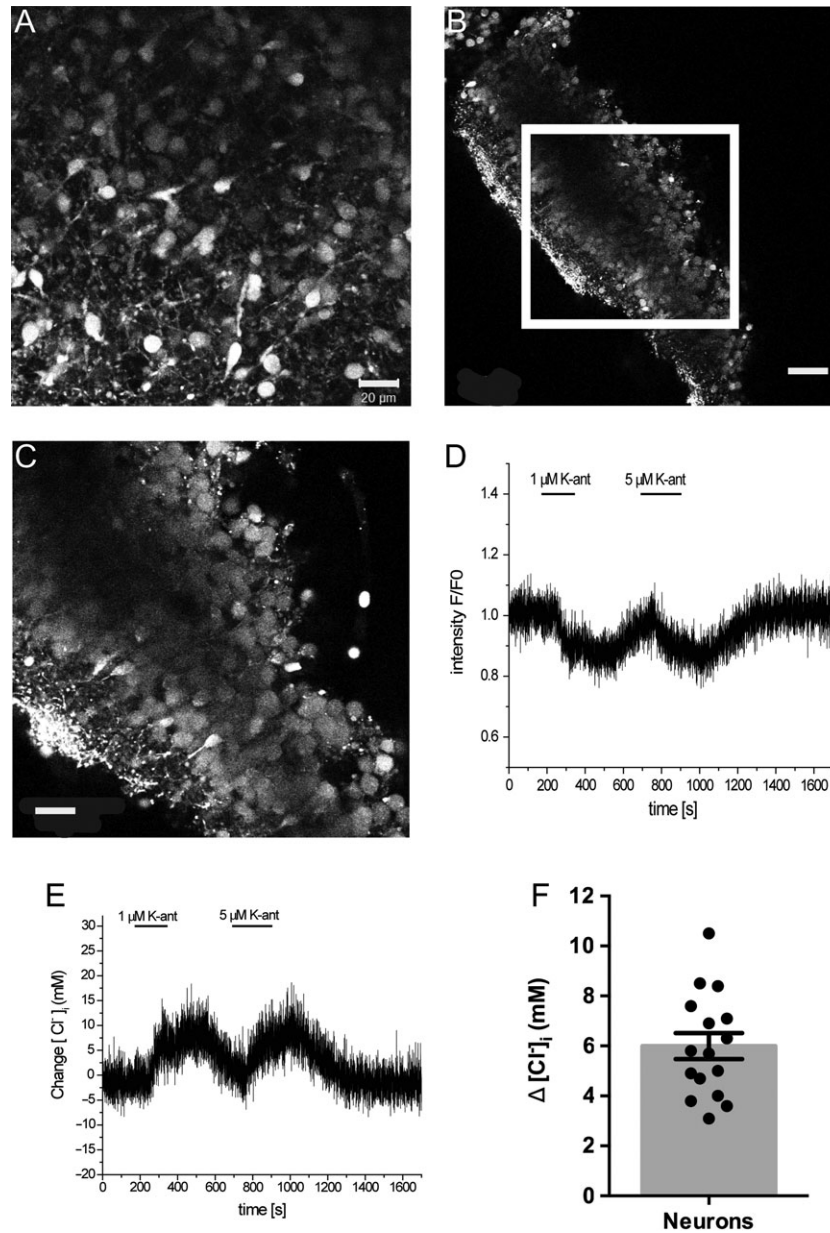
Figure 4. Effect of KCC2 antagonist on intracellular chloride concentration. (A) Shows neurons filled with MEQ dye in organotypic slices. (B) The integrity of neurons taking up the dye remains intact after 15 min recording the fluorescence intensity (without treatment); there is no bleaching effect and no leaking of dye out of cells; (C) shows the magnified white box in (B). (D) Fluorescence recording shows a drop in intensity and then recovery after washing out the antagonist. (E) This shows the estimation of the increase in intracellular chloride concentration corresponding to the trace in (D) using the Stern–Volmer equation; slices were treated with 1 and 5 μM concentrations of VU0240551. This shows inhibition of the KCC2 activity leading to transient increased intracellular $[Cl^-]$, and subsequent quenching of MEQ fluorescence intensity as expected. (F) Estimation of the increase in intracellular chloride concentration in 16 different neurons with an average plot. Scale = 20 μm for A and C and 50 μm for B.

Discussion

KCC2-NKCC1

The molecular mechanisms regulating the initiation, progress and termination of neuronal migration are numerous. The balance between excitation and inhibition in the neocortex is partially controlled by the KCC2-NKCC1-GABAergic system; NKCC1 is initially high, resulting in chloride import, which is eventually replaced by increased levels of KCC2, resulting in chloride export. This arrangement initially acts as a motogenic signal, encouraging neurons to move, and eventually as a stop signal, with the rise of KCC2, marking the termination of cortical migration (Bortone and Polleux 2009). Developmental manipulation of this system assists in understanding the role of these ion channel proteins in the progress and termination of cortical migration. KCC2 manipulation specifically influences GABA function during development and particularly affects cortical migration (Jablonska 2004; Cuzon et al. 2006; Bortone and Polleux 2009; Abbah and Juliano 2014). The developmental switch that results in the transformation of GABA from excitatory to inhibitory, due
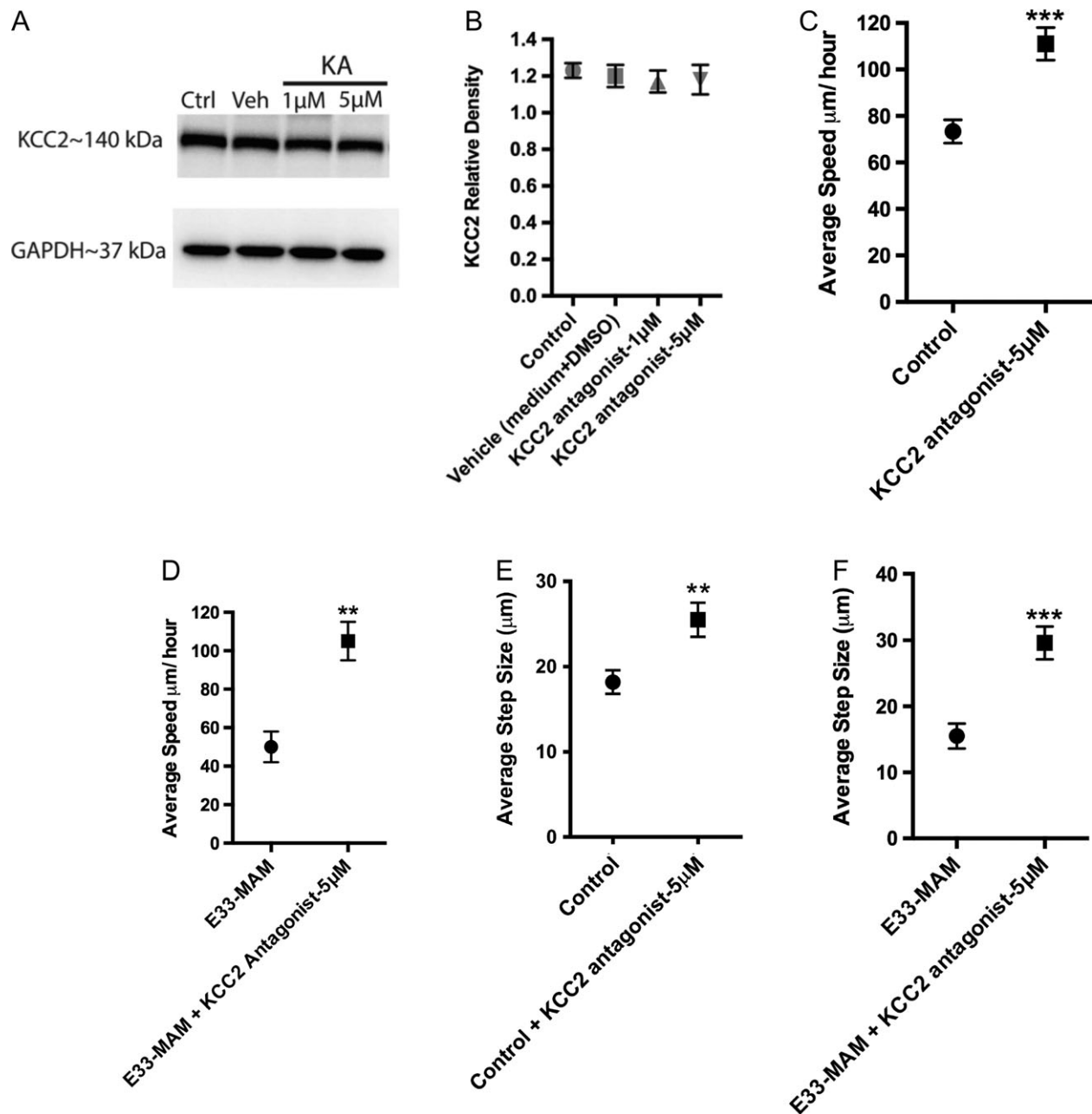
Figure 5. Effect of KCC2 antagonist treatment on features of migrating neurons. (*A, B*) Treatment of organotypic slices with VU0240551 for 5 h has no effect on KCC2 protein levels, shown in a western blot in (*A*); (*B*) is the quantification of western blots obtained for 3 animals for each group, showing no significant changes for control (Ctrl), medium + DMSO (Veh), addition of 1 and 5 μM concentrations of the KCC2 antagonist, VU240551. (*C, D*) Treatment of organotypic slices with VU0240551 significantly increases the speed of migrating neurons for both normal and E33 MAM treated slices; the data to extract speed data was obtained over the first 5 h of neuronal migration. (*E, F*) Treatment of organotypic cultures with VU0240551 also increases the step size of migrating neurons significantly for the first 5 h, Student's t-test, **$P < 0.01$, ***$P < 0.001$ (*E, F*). $N = 80$ neurons (Control), 74 neurons (Control + KCC2 antagonist), 5 neurons (E33 MAM Control), 22 neurons (E33 MAM + KCC2 antagonist).

to changes in the ratio of KCC2 and NKCC1 is crucial to understanding neuronal development (Bortone and Polleux 2009). A precocious overexpression of KCC2 accelerates the perinatal chloride shift, which consequently slows down the speed of migrating neurons and eventually makes them pause (Bortone and Polleux 2009). In our model, gestational E33 MAM treatment causes an early upregulation of KCC2 that correlates with decreased speed as well as altered behavior of migrating interneurons in ferret neocortex (Abbah and Juliano 2014).

KCC2 Downregulation With BPA Increases the Speed and Step Size of Migrating Interneurons Leaving the GE

BPA is an estrogenic chemical used in making polycarbonate and epoxy resins lining food and beverage cans and bottles. It belongs to the bisphenol family of compounds comprising, but not limited to, bisphenol B, C, E, and F. BPA is a potential gene toxicant during embryonic development and exposure can result in diverse adverse effects on human and animal health.
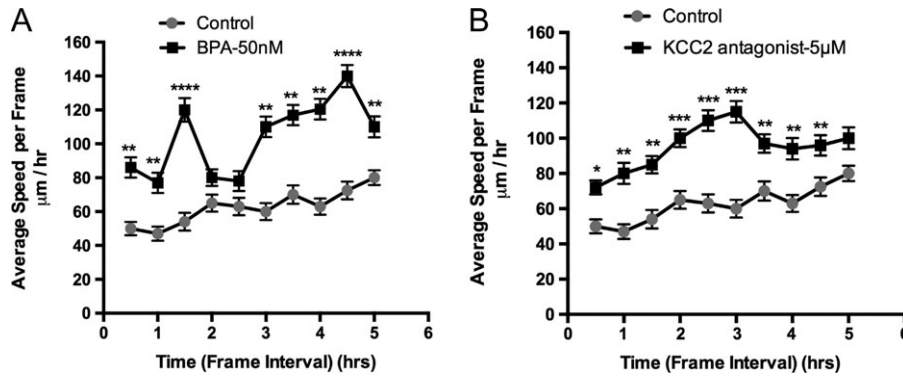
Figure 6. Variation of migration speed over the first 5 h of the migration assay. (A) After BPA treatment, the migration speed of electroporated neurons in organotypic cultures shows an overall increase over a period of 5 h. The speed varies considerably but shows a general increase over the 5 h period. For labeled neurons in the control slices, the trend also shows a general increase in speed over the 5 h period. The migration speed after addition of BPA is significantly higher than that of control neurons at all time points except between 2 and 3 h of measurement; 2-Way ANOVA, row factor $F(9, 1460) = 13.6$ followed by a Sidak post hoc test **$P < 0.01$, ****$P < 0.0001$. (B) After treatment with the KCC2 antagonist, the speed of migration shows a general increase for the 5 h period, with a peak at 3 h. The migration speed for labeled neurons with the added KCC2 antagonist is significantly higher than that of control at all time points except the last. Two-way ANOVA, row factor, $F(9, 1520) = 7.9$ followed by a Sidak post hoc test, *$P < 0.05$, ***$P < 0.001$, ****$P < 0.0001$. $N = 80$ neurons for Control, 63 neurons for KCC2 antagonist and 38 neurons for BPA.

These incorporate wide-ranging effects that include isolation behavior of babies from mothers in nonhuman primates as well as reduced overall exploration of their environment (Nakagami et al. 2009). Other experiments report endocrine disruptions leading to obesity (Vom Saal et al. 2012) and decreased fertility and fecundity in CD-1 mice (Cabaton et al. 2011). More directly related to neuronal development, several studies report abnormal cortical development when pregnant animals receive BPA during gestation. Relevant findings include acceleration of corticogenesis and an altered laminar pattern (Itoh et al., 2012; Komada et al. 2012, 2014). These specific effects on the cerebral cortex may be a direct result of the increased migratory speed we see in our current study. We note that manipulation of KCC2 appears to rescue the speed of neurons in MAM-treated organotypic cultures to the speed of BPA treatment alone (Fig. 2C,D) and not to an intermediate point. This may be because the manipulation of KCC2 by MAM on one hand and BPA on the other were not titrated to ensure application of equivalent amounts of both chemicals. The extent to which the dose of MAM (14 mg/kg body weight) upregulates KCC2 is not exactly opposite of the extent to which BPA (50 nM) downregulates KCC2. We therefore do not expect BPA exposure to equally cancel or nullify the action of MAM. Second, each drug was delivered with different routes of administration, we administered MAM in utero whereas BPA was administered in vitro on organotypic slices. This could also account for any dose differences. Given that MAM and BPA have opposite effects on KCC2 expression, we wanted to investigate whether their effect on speed and other features of migrating neurons would also be opposite (but not necessarily equal). Our results show that the opposite effect persists and affects the speed and other features (step size and number of turns) of migrating neurons.

Both prenatal and in-vitro exposure of neurons to BPA downregulate KCC2 mRNA and protein through epigenetic modifications, thereby delaying the KCC2 driven perinatal chloride shift and consequently increasing the speed of migrating interneurons in the neocortex (Yeo et al. 2013). This agrees with our finding that BPA treatment downregulates KCC2 and consequently increases the speed of migrating neurons leaving the GE in ferret neocortex. We also show that migrating neurons treated with BPA increase their step size as compared with control. Increased speed and step size implies movement over a longer distance than normal, which in terms of neuronal migration could lead to misplacements of neurons (cortical dysplasia) and consequent abnormal function of the brain. Our findings reveal that the perinatal chloride shift controlled by KCC2 is an important component influencing the speed and pattern of migrating neurons. Generally migrating neurons slow down and eventually stop moving when they differentiate and mature to assume the right position for normal function. The delay in perinatal chloride shift (caused by BPA treatment in our case) may delay the maturation time window and also maintains the GABAergic system in a depolarized state favorable for neuronal motility through calcium mediated activation of the cytoskeleton (through the voltage sensitive calcium channels, VSCC) in the normal slices (Behar et al. 1996; Heck et al. 2007; Bortone and Polleux 2009). The increase in speed and step size may be suggestive of a stronger depolarization effect leading to accentuated calcium mediated activation of the cytoskeleton through the VSCC, pending further investigations. In the case of the MAM treated slices, treatment with BPA provides an influence that suggests a reversal of the effect of MAM, resulting in increased migration speed than when treated with MAM alone. We found earlier that E33 MAM treated neurons were less exploratory by making fewer turns than controls (Abbah and Juliano 2014) indicating that abnormal KCC2 upregulation in our model probably impeded the cues, sense of orientation, and direction of migrating neurons. Our current finding shows that BPA treatment significantly increases the number of turns made by migrating neurons per hour compared with control. This suggests that KCC2 may play a role in neuronal guidance during migration as well (Lopez-Bendito et al. 2006).

The action of BPA in KCC2 downregulation occurs through epigenetic modification (methylation) of the KCC2 gene (Yeo et al. 2013). This global mechanism may not be specific to KCC2 and could possibly affect the expression of other genes involved in regulating neuronal migration. We are therefore cautious not to attribute the alterations in features of migration solely to KCC2 downregulation since other unknown players could be involved. As a result, we evaluated the effect of manipulating KCC2 levels with a pharmacologic antagonist.

To partially determine the relationship of the effects of increased KCC2 and other substances, we tested whether MAM-treated brains showed altered levels of the CpG binding

protein, MeCP2. KCC2 and MeCP2 are highly interrelated and KCC2 is most likely a downstream target of MeCP2 (Tang et al. 2016). Our finding that increased overall DNA methylation also occurs in MAM treated brains suggests that the increased levels of KCC2 follow as a result of increased overall methylation leading to increased MeCP2. This study, however, targets the specific effects of KCC2 by blocking its actions through antagonism, or by reducing its level. Since MeCP2 is often associated with features of neural development, future studies may attempt to manipulate MeCP2 to determine the effect of altering these levels on parameters similar to those evaluated here.

Inhibition of KCC2 Activity by the Antagonist VU0240551

The use of VU0240551 enabled us to specifically inhibit the activity of KCC2 without affecting NKCC1 and other anion channels, thereby enabling assessment of the specific effect of reducing KCC2 activity on features of migrating neurons. This KCC2 antagonist, VU0240551, selectively inhibits KCC2 by binding competitively to the K^+ site and noncompetitively to the Cl^- site in the KCC2 active region and impairing chloride movement (Delpire et al. 2009; Deisz et al. 2014). This manipulation in our hands, resulted in an increase in intracellular chloride concentration ranging from 3.1 to 10.5 mM. Given the physiologic levels of intracellular chloride concentration in neurons is about 4 mM, we are confident the estimated increase (~2–2.5-fold) is enough to alter KCC2 activity reflected in the variation of migration speed and step size. Here again, we show that inhibition of KCC2 activity correlates with an increase in speed and step size of migrating neurons leaving the GE, suggesting that interference with KCC2 alters neuronal migration. Blocking chloride channels delays the rate of chloride extrusion, which may delay the GABA polarity switch leading to an increase in speed and step size of migrating neurons most likely through the VSCC. Application of the KCC2 antagonist to E33 MAM slices significantly increases the average speed over that of MAM treated slices alone. It is clear that inhibiting the activity of KCC2 (either by BPA, which reduces the production of KCC2 protein, or by a specific pharmacologic antagonist) increases the speed of migrating neurons and also restores at least some exploratory behavior.

Variable Speed of Migrating Neurons Over Time

The speed of migrating neurons for both normal slices and those treated to decrease KCC2 tends to increase over the initial 5 h of recording. Since these values represent the average of all the cells we measured, obvious variability occurred among neurons. In addition, we only measure those cells that were moving continuously for 5 h; many neurons moved intermittently. Nevertheless, the overall trend for moving neurons shows increased speed. This suggests that the migrating cells are healthy and not adversely affected by being in culture or under the drug treatment. It is not clear why the speed increases over this period of time but it may represent a decrease in conflicting signals present in the organotypic culture. In addition, the speed of neurons in slices treated with BPA and the KCC2 antagonist is generally increased from the time we began evaluating their movements. There are some time points that show decreases in the average speed but these are mostly likely due to the overall variability of response. It is not clear what factors account for the observed pattern of variability of the speed in this case and understanding of the detailed mechanisms requires further investigation.
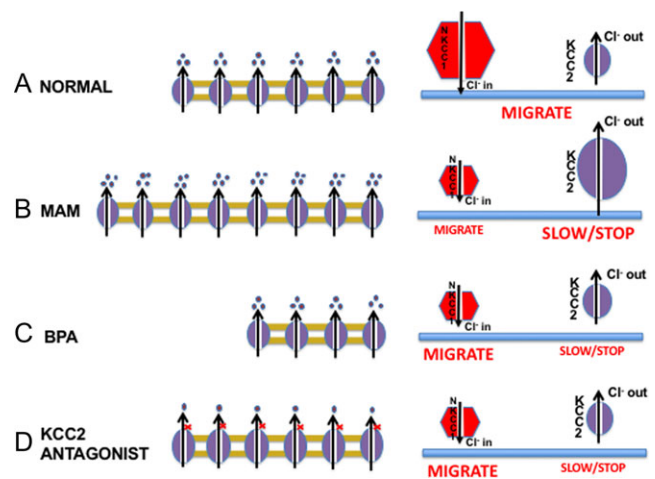

Figure 7. Model of KCC2 manipulation. (A) Normal KCC2 activity in balance with NKCC1 results in a polarity switch at the right time during development, causing neurons to migrate at the appropriate speed. During development, NKCC1 levels are higher than KCC2 levels. (B) E33 MAM treatment increases the KCC2 level, which hastens the polarity switch thereby slowing down migrating neurons. (C) BPA treatment reduces the amount of KCC2 protein and causes a delay in the polarity switch and stimulation of neuronal motility leading to increased speed. (D) The KCC2 antagonist, VU0240551, inhibits KCC2 activity, which results in a delay in the polarity switch and stimulation of neuronal motility leading to increased migration speed.

Conclusion

KCC2 is a chloride exporter and NKCC1 is a chloride importer. In young neurons, the expression of NKCC1 is higher relative to KCC2 leading to a greater intracellular chloride concentration making GABA depolarizing. As the neurons mature, the expression of KCC2 becomes increased relative to NKCC1, leading to a higher extracellular chloride concentration making GABA hyperpolarizing. The switch of GABA polarity from depolarizing to hyperpolarizing is precisely regulated by the balance of KCC2 and NKCC1, which contributes to factors regulating motility of migrating interneurons in the cortex. The switch in GABA polarity influences the motility of migrating neurons by stimulating the cytoskeleton through the VSCCs. A precocious upregulation of KCC2 through MAM treatment may hasten the polarity switch to hyperpolarization, which slows down neuronal motility, whereas a precocious downregulation of KCC2 through pharmacologic treatment delays the polarity switch extending depolarization, which may stimulate neuronal motility.

Figure 7 shows a cartoon of KCC2 manipulation in our experiments. (A) Shows that under normal conditions, the balance of KCC2 and NKCC1 results in a migration pattern where neurons migrate at a normal speed and reach the appropriate destination at the right time. At young ages, when neurons are migrating, the level of NKCC1 should be greater than that of KCC2. (B) Represents regulation of neuronal motility under MAM treatment where precocious KCC2 upregulation hastens the GABA polarity switch and slows migrating neurons. In (C) KCC2 expression is downregulated by BPA treatment. Under this condition, decreased KCC2 protein is produced and reduces the overall amount of available KCC2 leading to a delay in the polarity switch causing a longer depolarization time window and stimulating neuronal motility. In (D), a deficiency in the overall activity of KCC2 protein due to inhibition by the KCC2 antagonist (VU0240551) exists and leads to a reduction in chloride ion export causing a delay in polarity switch and consequent stimulation of neuronal motility.

Both KCC2 downregulation and interference with KCC2 activity have a similar effect on migrating neurons. BPA downregulates KCC2 expression leading to fewer KCC2 molecules, whereas the antagonist blocks normal function reducing overall KCC2 activity. BPA acts longer and affects gene expression, whereas the KCC2 antagonist is target specific and more focal, causing a more succinct functional outcome.

The use of MAM, on one hand, and BPA and VU0240551 on the other, are both cases of KCC2 manipulation indicating that an alteration in the perinatal chloride shift during brain development leads to abnormal neuronal migration. Understanding how they influence KCC2 enhances our understanding of the actions of KCC2 and its role in neuronal migration.

Supplementary Material

Supplementary material is available at *Cerebral Cortex* online.

Funding

Note

References

Abbah J, Braga MF, Juliano SL. 2014. Targeted disruption of layer 4 during development increases GABAA receptor neurotransmission in the neocortex. J Neurophysiol. 111:323–335.

Abbah J, Juliano SL. 2014. Altered migratory behavior of interneurons in a model of cortical dysplasia: the influence of elevated GABAA activity. Cereb Cortex. 24:2297–2308.

Bartolini F, Andres-Delgado L, Qu X, Nik S, Ramalingam N, Kremer L, Alonso MA, Gundersen GG. 2016. An mDia1-INF2 formin activation cascade facilitated by IQGAP1 regulates stable microtubules in migrating cells. Mol Biol Cell. 27: 1797–1808.

Behar TN, Li YX, Tran HT, Ma W, Dunlap V, Scott C, Barker JL. 1996. GABA stimulates chemotaxis and chemokinesis of embryonic cortical neurons via calcium-dependent mechanisms. J Neurosci. 16:1808–1818.

Ben-Ari Y. 2014. The GABA excitatory/inhibitory developmental sequence: a personal journey. Neuroscience. 279:187–219.

Ben-Ari Y, Cherubini E, Corradetti R, Gaiarsa JL. 1989. Giant synaptic potentials in immature rat CA3 hippocampal neurones. J Physiol. 416:303–325.

Biwersi J, Verkman AS. 1991. Cell-permeable fluorescent indicator for cytosolic chloride. Biochemistry. 30:7879–7883.

Bortone D, Polleux F. 2009. KCC2 expression promotes the termination of cortical interneuron migration in a voltage-sensitive calcium-dependent manner. Neuron. 62:53–71.

Cabaton NJ, Wadia PR, Rubin BS, Zalko D, Schaeberle CM, Askenase MH, Gadbois JL, Tharp AP, Whitt GS, Sonnenschein C, et al. 2011. Perinatal exposure to environmentally relevant levels of bisphenol A decreases fertility and fecundity in CD-1 mice. Environ Health Perspect. 119:547–552.

Cuzon VC, Yeh PW, Cheng Q, Yeh HH. 2006. Ambient GABA promotes cortical entry of tangentially migrating cells derived from the medial ganglionic eminence. Cereb Cortex. 16: 1377–1388.

Deisz RA, Wierschke S, Schneider UC, Dehnicke C. 2014. Effects of VU0240551, a novel KCC2 antagonist, and DIDS on chloride homeostasis of neocortical neurons from rats and humans. Neuroscience. 277:831–841.

Delpire E. 2000. Cation-chloride cotransporters in neuronal communication. News Physiol Sci. 15:309–312.

Delpire E, Days E, Lewis LM, Mi D, Kim K, Lindsley CW, Weaver CD. 2009. Small-molecule screen identifies inhibitors of the neuronal K-Cl cotransporter KCC2. Proc Natl Acad Sci USA. 106:5383–5388.

Fishell G, Kriegstein A. 2005. Cortical development: new concepts. Neuron. 46:361–362.

Flames N, Long JE, Garratt AN, Fischer TM, Gassmann M, Birchmeier C, Lai C, Rubenstein JL, Marin O. 2004. Short- and long-range attraction of cortical GABAergic interneurons by neuregulin-1. Neuron. 44:251–261.

Gal JS, Morozov YM, Ayoub AE, Chatterjee M, Rakic P, Haydar TF. 2006. Molecular and morphological heterogeneity of neural precursors in the mouse neocortical proliferative zones. J Neurosci. 26:1045–1056.

Hatten ME. 2002. New directions in neuronal migration. Science. 297:1660–1663.

Heck N, Kilb W, Reiprich P, Kubota H, Furukawa T, Fukuda A, Luhmann HJ. 2007. GABA-A receptors regulate neocortical neuronal migration in vitro and in vivo. Cereb Cortex. 17:138–148.

Inglefield JR, Schwartz-Bloom RD. 1999. Fluorescence imaging of changes in intracellular chloride in living brain slices. Methods. 18:197–203.

Itoh K, Yaoi T, Fushiki S. 2012. Bisphenol A, an endocrine-disrupting chemical, and brain development. Neuropathology. 32:447–457.

Jablonska B. 2004. GABAA receptors reorganize when layer 4 in ferret somatosensory cortex is disrupted by methylazoxymethanol (MAM). Cereb Cortex. 14:432–440.

Kahle KT, Staley KJ, Nahed BV, Gamba G, Hebert SC, Lifton RP, Mount DB. 2008. Roles of the cation-chloride cotransporters in neurological disease. Nat Clin Pract Neurol. 4:490–503.

Komada M, Asai Y, Morii M, Matsuki M, Sato M, Nagao T. 2012. Maternal bisphenol A oral dosing relates to the acceleration of neurogenesis in the developing neocortex of mouse fetuses. Toxicology. 295:31–38.

Komada M, Itoh S, Kawachi K, Kagawa N, Ikeda Y, Nagao T. 2014. Newborn mice exposed prenatally to bisphenol A show hyperactivity and defective neocortical development. Toxicology. 323:51–60.

Krapf R, Berry CA, Verkman AS. 1988. Estimation of intracellular chloride activity in isolated perfused rabbit proximal convoluted tubules using a fluorescent indicator. Biophys J. 53: 955–962.

Lopez-Bendito G, Cautinat A, Sanchez JA, Bielle F, Flames N, Garratt AN, Talmage DA, Role LW, Charnay P, Marin O, et al. 2006. Tangential neuronal migration controls axon guidance: a role for neuregulin-1 in thalamocortical axon navigation. Cell. 125:127–142.

Lu J, Karadsheh M, Delpire E. 1999. Developmental regulation of the neuronal-specific isoform of K-Cl cotransporter KCC2 in postnatal rat brains. J Neurobiol. 39:558–568.

Marin O. 2003. Directional guidance of interneuron migration to the cerebral cortex relies on subcortical Slit1/2-independent repulsion and cortical attraction. Development. 130:1889–1901.

Marin O, Rubenstein JL. 2003. Cell migration in the forebrain. Annu Rev Neurosci. 26:441–483.

Marin O, Valiente M, Ge X, Tsai LH. 2010. Guiding neuronal cell migrations. Cold Spring Harb Perspect Biol. 2:a001834.

Miyoshi G, Fishell G. 2011. GABAergic interneuron lineages selectively sort into specific cortical layers during early postnatal development. Cereb Cortex. 21:845–852.

Mueller AL, Taube JS, Schwartzkroin PA. 1984. Development of hyperpolarizing inhibitory postsynaptic potentials and hyperpolarizing response to gamma-aminobutyric acid in rabbit hippocampus studied in vitro. J Neurosci. 4: 860–867.

Nakagami A, Negishi T, Kawasaki K, Imai N, Nishida Y, Ihara T, Kuroda Y, Yoshikawa Y, Koyama T. 2009. Alterations in male infant behaviors towards its mother by prenatal exposure to bisphenol A in cynomolgus monkeys (Macaca fascicularis) during early suckling period. Psychoneuroendocrinology. 34: 1189–1197.

Negri-Cesi P. 2015. Bisphenol A interaction with brain development and functions. Dose Response. 13:1559325815590394.

Palmer SL, Noctor SC, Jablonska B, Juliano SL. 2001. Laminar specific alterations of thalamocortical projections in organotypic cultures following layer 4 disruption in ferret somatosensory cortex. Eur J Neurosci. 13:1559–1571.

Poluch S, Drian MJ, Durand M, Astier C, Benyamin Y, Konig N. 2001. AMPA receptor activation leads to neurite retraction in tangentially migrating neurons in the intermediate zone of the embryonic rat neocortex. J Neurosci Res. 63:35–44.

Poluch S, Juliano SL. 2015. 'Fine-tuning of neurogenesis is essential for the evolutionary expansion of the cerebral cortex'. Cereb Cortex. 25:346–364.

Poluch S, Rossel M, Konig N. 2003. AMPA-evoked ion influx is strongest in tangential neurons of the rat neocortical intermediate zone close to the front of the migratory stream. Dev Dyn. 227:416–421.

Puskarjov M, Ahmad F, Kaila K, Blaesse P. 2012. Activity-dependent cleavage of the K-Cl cotransporter KCC2 mediated by calcium-activated protease calpain. J Neurosci. 32:11356–11364.

Rakic P. 2009. Evolution of the neocortex: a perspective from developmental biology. Nat Rev Neurosci. 10:724–735.

Rudolph J, Zimmer G, Steinecke A, Barchmann S, Bolz J. 2014. Ephrins guide migrating cortical interneurons in the basal telencephalon. Cell Adh Migr. 4:400–408.

Schwartz RD, Yu X. 1995. Optical imaging of intracellular chloride in living brain slices. J Neurosci Methods. 62:185–192.

Verkman AS. 1990. Development and biological applications of chloride-sensitive fluorescent indicators. Am J Physiol. 259: C375–C388.

Vom Saal FS, Nagel SC, Coe BL, Angle BM, Taylor JA. 2012. The estrogenic endocrine disrupting chemical bisphenol A (BPA) and obesity. Mol Cell Endocrinol. 354:74–84.

Yeo M, Berglund K, Hanna M, Guo JU, Kittur J, Torres MD, Abramowitz J, Busciglio J, Gao Y, Birnbaumer L, et al. 2013. Bisphenol A delays the perinatal chloride shift in cortical neurons by epigenetic effects on the Kcc2 promoter. Proc Natl Acad Sci USA. 110:4315–4320.